Structural and X-ray spectroscopy studies of $Pb_{1-x}Ba_x(NO_3)_2$ solid solutions

L.I. Isaenko [a,b], K.E. Korzhneva [a,b], O.Y. Khyzhun [c,*], M.S. Molokeev [d], A.A. Goloshumova [a,b], A.Y. Tarasova [b]

[a] *Novosibirsk State University, 630090, Novosibirsk, Russia*
[b] *V.S. Sobolev Institute of Geology and Mineralogy, SB RAS, 630090, Novosibirsk, Russia*
[c] *Frantsevych Institute for Problems of Materials Science, National Academy of Sciences of Ukraine, 3 Krzhyzhanivsky Street, UA-03142, Kyiv, Ukraine*
[d] *Kirensky Institute of Physics Federal Research Center KSC SB RAS, Krasnoyarsk, 660036, Russia*

ARTICLE INFO

ABSTRACT

$Pb_{0.75(3)}Ba_{0.25(3)}(NO_3)_2$, $Pb_{0.68(3)}Ba_{0.32(3)}(NO_3)_2$, $Ba_{0.58(3)}Pb_{0.42(3)}(NO_3)_2$, $Ba_{0.81(3)}Pb_{0.19(3)}(NO_3)_2$ crystals were grown for the first time when studying the $Pb(NO_3)_2$–$Ba(NO_3)_2$–H_2O system. The crystals were grown in water solution with different relation of $Pb(NO_3)_2$ and $Ba(NO_3)_2$. It was found that series of solid solutions were formed by interaction of simple $Pb(NO_3)_2$ and $Ba(NO_3)_2$ compounds with a slow increase of volume and cell parameters from pure lead nitrate to pure barium nitrate. The crystal structure of all obtained $Pb_{1-x}Ba_x(NO_3)_2$ crystals belong to a cubic space group Pa-3. In these structures, Pb and Ba cations have the same coordination number 12, but different ionic radii (1.49 and 1.61 Å, respectively), anionic group is an equilateral triangle with O–O–O angle of 60° and O–O bond lengths ranging from 2.1305(8) to 2.2585(7) Å. The Pb^{2+} ion has a lone pair of electrons that are likely to be stereochemically active in these solid solutions leading to a significant amount of local disorder which explains the spread in the lattice parameters. The $Pb_{1-x}Ba_x(NO_3)_2$ solid solutions were characterized by X-ray photoelectron spectroscopy (XPS) by measuring the binding energies of the core-levels of constituting atoms and the shapes of the valence band. The XPS measurements indicate that the substitution of Pb for Ba does not cause changes in the charge states of the atoms constituting the $Pb_{1-x}Ba_x(NO_3)_2$ crystals. Matching the XPS valence-band spectra and the X-ray emission O Kα bands on a common energy scale indicates that the principal contributions of O 2p states occur at the top of the valence band of the crystals under study with also their substantial input in the upper and central portions of the band.

1. Introduction

The need for effective crystalline functional materials is constantly increasing with the progress of high technologies. Therefore, the development of principles and methods of the search for these compounds is an important and actual problem of the materials science. To determine the mechanism of formation of new compounds with the particular characteristics, it is reasonable to study the influence of composition changes on crystal structure and properties in the certain system. The well-known method of search for new compounds is based on a change of composition. Usually, the series of compounds are examined and the regularities between their composition–structure–properties are established. It is known that nitrates are characterized by the stability of the NO_3 group unlike carbonates and borates that form a variety of rings and chains. The radii and valences of the cations play a major role in the formation of new double nitrate compounds and make different effects on crystal structural motifs and properties. A large number of crystals with cations having different radii and valences are known for these compounds [1–3]. Research on new systems with cation structure design allows to obtain and study new functional materials with given properties and makes a great interest for fundamental investigations of phase formation.

According to McMurdie et al. [4], $Pb_{0.67}Ba_{0.33}(NO_3)_2$ and $Pb_{0.33}Ba_{0.67}(NO_3)_2$ compounds found in the $Pb_{1-x}Ba_x(NO_3)_2$ system belong to cubic noncentrosymmetric structure ($P2_13$), but Shtukenberg et al. [5] described a solid solution of $Pb_{1-x}Ba_x(NO_3)_2$ composition with trigonal centrosymmetric structure (R-3). In this paper a structural study and X-ray spectroscopy measurements were made in order to investigate the influence of divalent cations on the crystal and electronic structures of the series of $Pb_{1-x}Ba_x(NO_3)_2$ solid solutions.

2. Experimental

$Pb(NO_3)_2$ (99.99%), $Ba(NO_3)_2$ (99.98%) and distilled water were used as initial materials to obtain $Pb_{1-x}Ba_x(NO_3)_2$ crystals.

Several series of experiments with the ratio of $Pb(NO_3)_2$:-$Ba(NO_3)_2 = 8:2$, 7:3, 6:4, 5:5, 4:6 and 3:7 were carried out. All experiments were performed under the same conditions. The crystals were grown in a water crystallizer by mixing powders of $Pb(NO_3)_2$ and $Ba(NO_3)_2$ in certain ratios and, then, dissolving them in water at temperature of 75 °C. Crystal growth was carried out by slow cooling at a rate of 1 °C/day in the temperature range from 75 to 45 °C and low evaporation. Crystals from 0.2 to 1 cm in size were obtained after a month of growth. Their stoichiometric formulas at a ratio of $Pb(NO_3)_2$ to $Ba(NO_3)_2$ are as follows: 8:2 – $Pb_{0.75(3)}Ba_{0.25(3)}(NO_3)_2$; 7:3 – $Pb_{0.68(3)}Ba_{0.32(3)}(NO_3)_2$; 6:4 – $Ba_{0.58(3)}Pb_{0.42(3)}(NO_3)_2$; 5:5 – $Ba_{0.81(3)}Pb_{0.19(3)}(NO_3)_2$.

The powder diffraction data for Rietveld analysis were collected at room temperature using a Bruker D8 ADVANCE powder diffractometer (Cu-Kα radiation) and a linear VANTEC detector. The step size of 2θ was 0.016°. The 2θ range of 5-70° was measured with a 0.6 mm divergence slit and with the counting time of 1.2 s per step. Rietveld refinements were performed using TOPAS 4.2 [6].

To define the atomic content and peculiarities of the chemical bonding in the $Pb_{1-x}Ba_x(NO_3)_2$ crystals, we have employed a possibility of X-ray photoelectron spectroscopy (XPS) as realized in the UHV-Analysis-System produced by SPECS Surface Nano Analysis Company (Germany). The present XPS measurements of the $Pb_{1-x}Ba_x(NO_3)_2$ crystals were carried out following the technique used earlier for similar studies of the electronic structure and features of the chemical bonding of the related compound $K_2Ba(NO_3)_4$ [1]. Briefly, the XPS spectra, both core-level and valence-band (VB), were excited by an X-ray Mg Kα source ($h\nu = 1253.6$ eV) and acquired at constant pass energy of 35 eV in a sublimation ion-pumped chamber of the UHV-Analysis-System possessing a residual pressure of about 6×10^{-8} Pa. The calibration technique was the same as reported elsewhere [1] and the charging drift was considered with the reference of the hydrocarbon XPS C 1s line to 284.6 eV as it is suggested for many-component nitrogen- and oxide-bearing compounds [1,7–9]. Furthermore, taking into account that in complex related many-component oxide-based materials [1,8–11] the principal input in the VB region is derived due to contributions of O 2p states, in the present work we employ also possibilities of ultra-soft X-ray emission spectroscopy (USXES) to measure the O Kα band ($L_{II,III} \rightarrow$ K transition) giving information on peculiarities of energy distribution of electronic states of the 2p-symmetry of oxygen [12]. In the present work, the technique of measuring the X-ray emission O Kα band of the $Pb_{1-x}Ba_x(NO_3)_2$ crystals was the same as it was applied for recording the band of related oxide material, $K_2Ba(NO_3)_4$ [1]. Briefly, we use the close operating conditions (accelerating voltage = 5600 V, anode current = 4.0 mA) and the same USXES equipment (RSM-500 spectrometer) as reported elsewhere [1].

3. Results and discussion

The goal of the present study was to identify the effect of Ba^{2+} and Pb^{2+} cations on the structural motifs of $Ba(NO_3)_2$, $Pb(NO_3)_2$ and Pb_{1-}

$_xBa_x(NO_3)_2$. For grown $Pb_{1-x}Ba_x(NO_3)_2$ crystals, refinements by the Rietveld method were performed and the stoichiometric formula of the compounds in this series were determined. All peaks were indexed within a cubic cell (Pa-3) with unit cell parameters close to that of $Ba(NO_3)_2$ [13], so that this crystal structure was taken as the starting model for the Rietveld refinement. The position of Ba in the structure was occupied by Pb^{2+} and Ba^{2+} ions, and the (Pb)/(Ba) ratio was refined with a linear constraint (Pb)+(Ba) = 1. Refinements were stable and low R-factors were obtained (Table 1). The lengths of the main bonds are listed in Table 2.
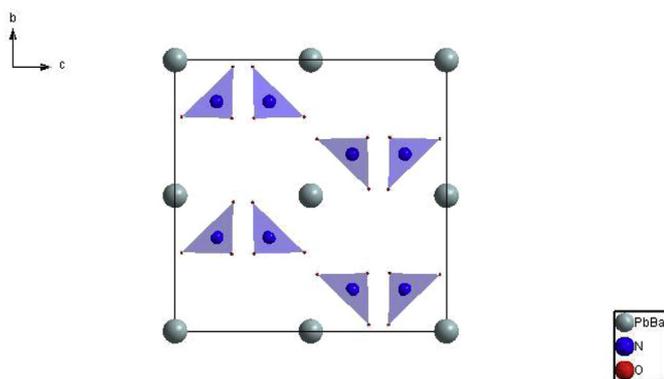
All obtained $Pb_{1-x}Ba_x(NO_3)_2$ crystals belong to a cubic syngony within a space group Pa-3 and with the parameter a ranging from 7.956(3) to 8.096(6) Å, while V ranging from 503.615(3) to 530.68(1) Å^3 (Table 1, Fig. 1). The structure has one nitrogen position and one oxygen position. Oxygen and nitrogen form an equilateral triangle in these compounds. The lengths of N–O and O–O bonds change from 1.221(1) to 1.306(6) Å and from 2.1305(8) to 2.2585(7) Å, respectively (Table 2). Lead and barium atoms (Pb/Ba) occupy the same position (coordination number 12) in the corners of the lattice and are reproduced by symmetry elements. Each unit cell contains eight NO_3 triangles and nine (Pb/Ba) atoms. The trend line in Fig. 2 shows the change in the cell volume in a series of $Pb_{1-x}Ba_x(NO_3)_2$ solid solutions (blue points). The volume of $Pb(NO_3)_2$ (left) and $Ba(NO_3)_2$ (right) are indicated by points, for comparison.

Comparison of grown crystals of the $Pb_{1-x}Ba_x(NO_3)_2$ series with pure $Ba(NO_3)_2$ and $Pb(NO_3)_2$ shows that there is a gradual increase in a and V cell parameters from $Pb(NO_3)_2$ to $Ba(NO_3)_2$ (Table 2). The O–O–O angle in the NO_3 triangle is equal to 60° in the crystals under consideration. It should be indicated that the Pb^{2+} ion has a lone pair of electrons that are likely to be stereochemically active in these solid solutions. This may lead to a significant amount of local disorder which explains the spread in the lattice parameters as discussed above. The effect of stereochemical activity of the '6s^2' lone pair of electrons is recognized on allowing the Pb^{2+} ion with partial occupancies to disorder near special crystallography positions as established by Moore et al. [14–16].
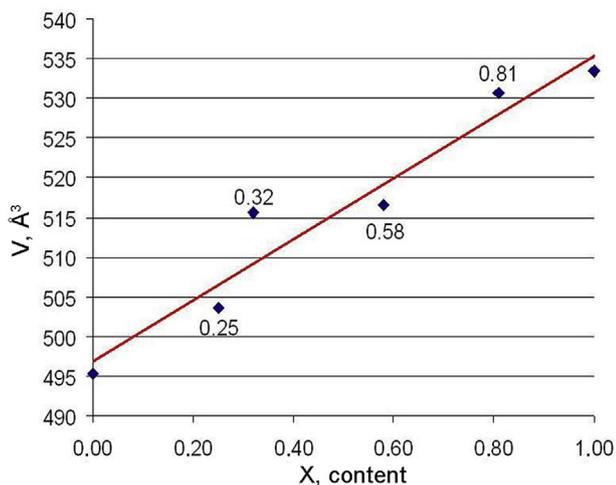
Furthermore, since the present $Pb_{1-x}Ba_x(NO_3)_2$ crystals were grown from water solutions, they are characterized by the kinetic of ordering of constituting atoms that is a unique phenomenon of solid solutions grown from aqueous solutions and it is called "growth ordering of atoms" or "growth dissymmetrization" [5,17]. Such an ordering was previously detected to exist in the case of about twenty compounds, in particular quartz crystals [18], mixed $NaCl_xBr_{1-x}O_3$ crystals of isomorphous salts of sodium chlorate, $NaClO_3$, and sodium bromate, $NaBrO_3$ [19–21], alums [22], topaz [23], garnets [24], strontium-lead nitrates $(Sr,Pb)(NO3)_2$ [5, 25]. The phenomenon of growth dissymmetrization in such crystals and their solid solutions is explained by the fact that strictly equivalent atomic positions in a crystal bulk are not equivalent geometrically and energetically near their surfaces [5]. Therefore, ordered distributions of isomorphous atoms in the topmost surface layers rise in such a case and ordering surface state can penetrate in the bulk during crystal growing [5,25]. In spite of the fact that this state is metastable, however, as a result of very slow diffusion rates, it can preserve for a long time in the crystal [5]. As a result, many such crystals (solid solutions) possess anomalous birefringence induced by the anion growth ordering [5,24, 25].

Table 1
The main results of the refinement by the Rietveld method for $Pb_{1-x}Ba_x(NO_3)_2$ crystals.

Compounds	$Pb_{0.75}Ba_{0.25}(NO_3)_2$	$Pb_{0.68}Ba_{0.32}(NO_3)_2$	$Pb_{0.42}Ba_{0.58}(NO_3)_2$	$Pb_{0.19}Ba_{0.81}(NO_3)_2$
Space group	Pa-3	Pa-3	Pa-3	Pa-3
a, Å	7.956(3)	8.019(8)	8.023(3)	8.096(6)
V, Å^3	503.615(3)	515.574(8)	516.492(5)	530.68(1)
R_{wp}, %	7.678	5.481	5.566	8.865
R_p, %	5.979	5.066	4.275	6.891
χ^2	2.361	2.556	3.651.	1.478
R_B, %	3.253	2.144	1.525	1.97

Table 2
Characteristics of NO₃ group in the series of the Pb₁₋ₓBaₓ(NO₃)₂ solid solutions.

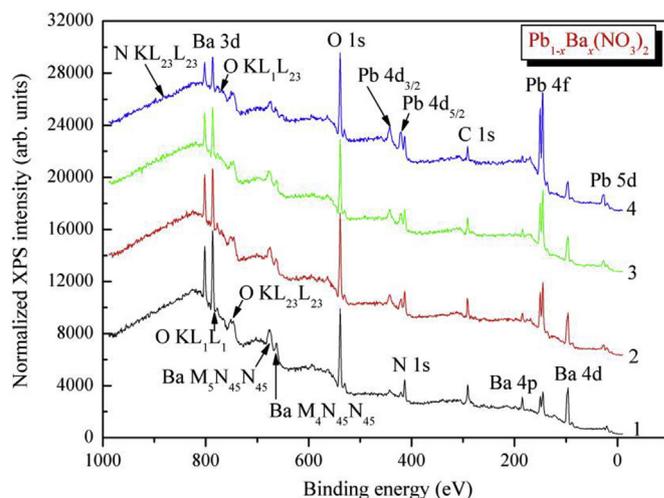|	Pb(NO₃)₂	Pb₀.₇₅Ba₀.₂₅.(NO₃)₂	Pb₀.₆₈Ba₀.₃₂. (NO₃)₂	Pb₀.₄₂Ba₀.₅₈. (NO₃)₂	Pb₀.₁₉Ba₀.₈₁.(NO₃)₂	Ba(NO₃)₂
a, Å	7.8586(2)	7.956(3)	8.019(8)	8.023(3)	8.096(6)	8.1102(1)
V, Å³	495.33(2)	503.615(3)	515.574(8)	516.492(5)	530.68(1)	533.45(3)
distance (Ba/Pb)₁–O	2.7482(6)	2.8037(8)	2.872(5)	2.8535(5)	2.8481(8)	2.8865(3)
distance (Ba/Pb)₂–O	2.8688(6)	2.8911(8)	2.8786(5)	2.8945(5)	2.9581(8)	2.9228(3)
distance N–O	1.2469(7)	1.2457(1)	1.232(7)	1.3057(7)	1.2207(1)	1.2611(6)
distance O–O	2.1597(8)	2.1572(1)	2.1305(8)	2.2585(4)	2.1023(1)	2.1589(7)

Fig. 1. The structure of the Pb₁₋ₓBaₓ(NO₃)₂ solid solution.

Fig. 2. The change in unit cell volume of the Pb₁₋ₓBaₓ(NO₃)₂ solid solutions.

Fig. 3. Survey XPS spectra of Pb₁₋ₓBaₓ(NO₃)₂ crystals: (1) Pb₀.₁₉Ba₀.₈₁(NO₃)₂, (2) Pb₀.₄₂Ba₀.₅₈(NO₃)₂, (3) Pb₀.₆₈Ba₀.₃₂(NO₃)₂ and (4) Pb₀.₇₅Ba₀.₂₅(NO₃)₂.

Survey XPS spectra of the Pb₁₋ₓBaₓ(NO₃)₂ crystals are presented in Fig. 3. All XPS features are well ascribed to the core-levels and Auger lines of the chemical elements constituting the Pb₁₋ₓBaₓ(NO₃)₂ crystals. The exception is only the C 1s line and it originates due to hydrocarbon surface adsorbates from laboratory air because we did not detect any shoulders positioned at its higher binding energy side that could be related to carbonate formation. However, as Fig. 3 presents, the relative intensities of the C 1s lines on the survey XPS spectra are comparatively low in the Pb₁₋ₓBaₓ(NO₃)₂ crystals under study. When going from Pb₀.₁₉Ba₀.₈₁(NO₃)₂ to Pb₀.₇₅Ba₀.₂₅(NO₃)₂ through the intermediate contents of the Pb₁₋ₓBaₓ(NO₃)₂ crystals, the relative intensities of the core-level XPS Ba 3d(4p,4d) spectra quietly decrease while those of the Pb 4d(4f,5d) spectra increase (see Figs. 3–5). Fig. 3 presents that the relative intensities of the XPS N 1s and O 1s lines do not alter when substituting lead for barium in the Pb₁₋ₓBaₓ(NO₃)₂ solid solutions. It is apparent that the XPS Ba 3d₅/₂ spectrum superimposes the Auger O KL₁L₁ line (Fig. 4a),

the N 1s line lays on the low-energy binding energy tail of the Pb 4d₅/₂ spectrum (Fig. 4c), while the superposition of the Pb 5d, Ba 5s and O 2s spectra (Fig. 5) is detected in the case of the present XPS measurements of the Pb₁₋ₓBaₓ(NO₃)₂ crystals under consideration.

As can be seen from the XPS spectra presented in Fig. 4 and data listed in Table 3, we do not observe any visible changes in magnitudes of the spin-orbit (SO) splitting of the XPS core-level Ba 3d(4d) and Pb 4d(4f) spectra when changing the compositions of the Pb₁₋ₓBaₓ(NO₃)₂ crystals from Pb₀.₁₉Ba₀.₈₁(NO₃)₂ to Pb₀.₇₅Ba₀.₂₅(NO₃)₂ through the intermediate contents. In the above sequence of compounds we do not detect any substantial changes in the binding energy values of the core electrons measured for the atoms constituting the Pb₁₋ₓBaₓ(NO₃)₂ crystals. Therefore, substitution of lead for barium do not lead to changes in the charge states of the atoms which constitute the Pb₁₋ₓBaₓ(NO₃)₂ crystals. As can be seen from Table 3, the present XPS measurements of the binding energies of the core-level electrons in the Pb₁₋ₓBaₓ(NO₃)₂ solid solutions are in fair agreement with those reported by Vasquez [26] for Ba(NO₃)₂ and Taylor et al. [27] for Pb(NO₃)₂. Somewhat higher binding energy values reported for Pb(NO₃)₂ is explained by the fact that the XPS data by Taylor et al. [27] are referenced to the C 1s line of hydrocarbons as 285.0 eV, while in the present work and in Ref. [26] the C 1s core-level spectrum is suggested to posses binding energy of 284.6 eV.

It should be indicated that binding energy values of the XPS N 1s core-level spectra of the Pb₁₋ₓBaₓ(NO₃)₂ solid solutions being in the range of (406.9–407.0)±0.1 eV (Table 3) are significantly bigger as compared with those of nitrides based on transition metals as well as inorganic nitrogen-containing compounds in which N 1s electrons binding energy is within 396.6–402.1 eV [28,29]. However, comparative high binding energies are found to be characteristic of other related nitrogen-bearing compounds, in particular K₂Ba(NO₃)₄ (406.9 eV [1]), Ba(NO₃)₂ (407.1 eV [26]), Pb(NO₃)₂ (407.4 eV [27]), KNO₃ and LiNO₃ (407.6 eV [30]), NH₄NO₃ (407.2 eV [31]), and NaNO₃ (407.3 eV [32]). Those big
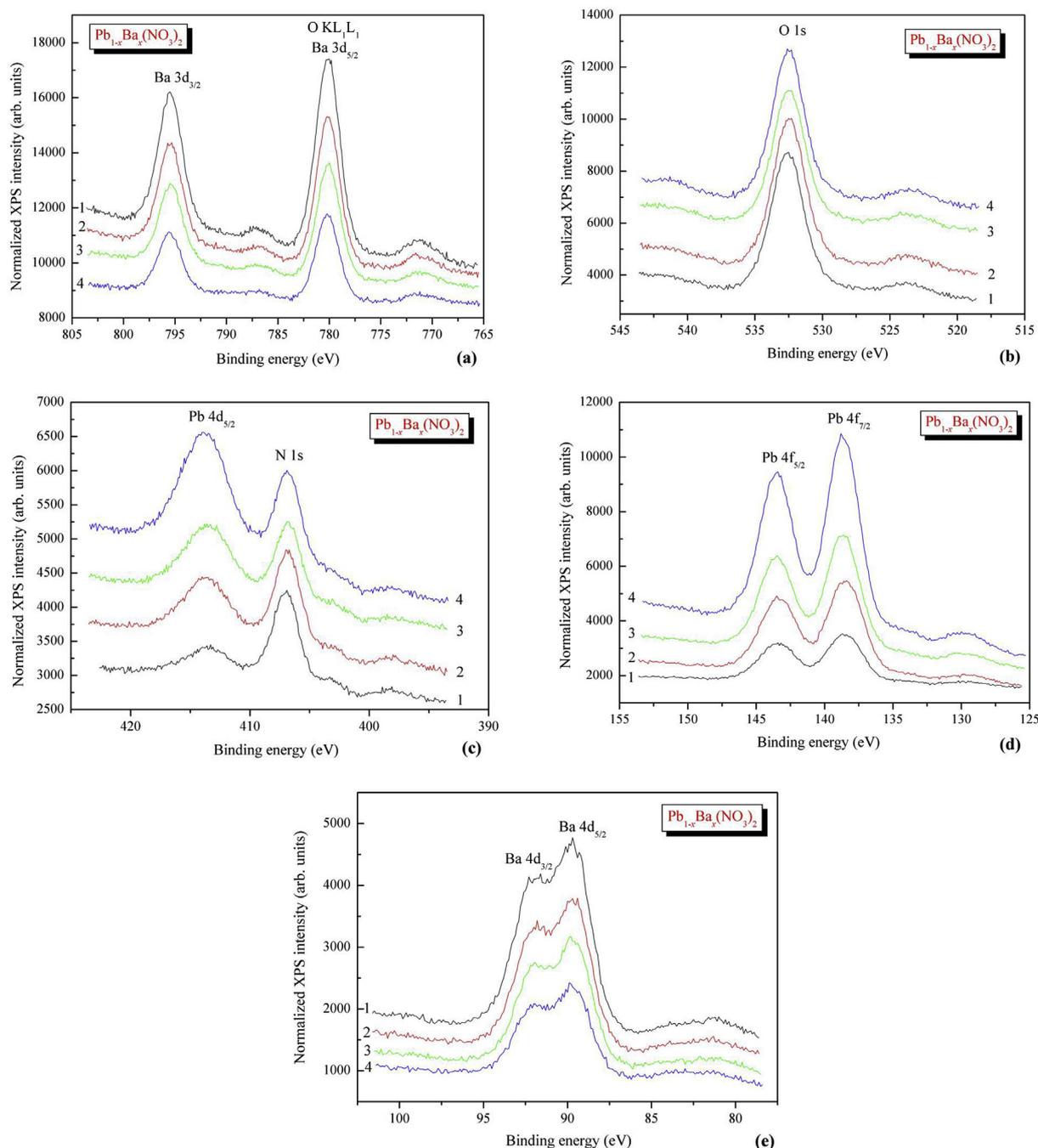
Fig. 4. XPS core-level (a) Ba 3d, (b) O 1s, (c) Pb $4d_{5/2}$ and N 1s, (d) Pb 4f, and (e) Ba 4d spectra of $Pb_{1-x}Ba_x(NO_3)_2$ crystals: (1) $Pb_{0.19}Ba_{0.81}(NO_3)_2$, (2) $Pb_{0.42}Ba_{0.58}(NO_3)_2$, (3) $Pb_{0.68}Ba_{0.32}(NO_3)_2$ and (4) $Pb_{0.75}Ba_{0.25}(NO_3)_2$.

binding energy magnitudes of the XPS N 1s core-level spectra are due to high charges located on N atoms in the mentioned nitrogen-bearing compounds [31]. The binding energy values of the XPS O 1s core-level spectra in the $Pb_{1-x}Ba_x(NO_3)_2$ solid solutions ((532.5–532.6)±0.1 eV, Table 3) are also much bigger as compared with those of the O 1s electrons in transition metal oxides (529.7–530.5 eV [28–30]) as well as in BaO (530.0 eV [26]) and PbO_2 (529.2 eV [27]).

It is worth mentioning that the $Pb_{1-x}Ba_x(NO_3)_2$ solid solutions can possess some nonstoichiometry. XPS is recognized a very powerful technique for nondestructive evaluating chemical composition of solids [28,29]; however, in the case of the solid solutions under study we can not do precise measurements of the elemental compositions because the binding energies of the O 1s electrons of bonding oxygen in them

(Table 3) superimpose those of the same electrons for oxygen-containing species adsorbed on the crystal surfaces [7,33,34] due to their exposure to laboratory air. When treating $Pb_{1-x}Ba_x(NO_3)_2$ crystal surfaces with 3 keV Ar^+ ions following the technique [1], simultaneously with surface cleaning, we detected also the preferential etching of oxygen and nitrogen atoms from topmost surface layers. Similar effect was detected previously when treating with Ar^+ ions the $K_2Ba(NO_3)_4$ crystal surface [1]. When using a cleaning technique with a diamond file following data of Ref. [35], we detected crystal crashing in every attempt due to high brittleness of the $Pb_{1-x}Ba_x(NO_3)_2$ crystals. Therefore, we leave a problem of $Pb_{1-x}Ba_x(NO_3)_2$ solid solution nonstoichiometry for future research.

In accordance with the results of band-structure calculations and/or X-ray spectroscopy studies of related oxygen- and nitrogen-bearing
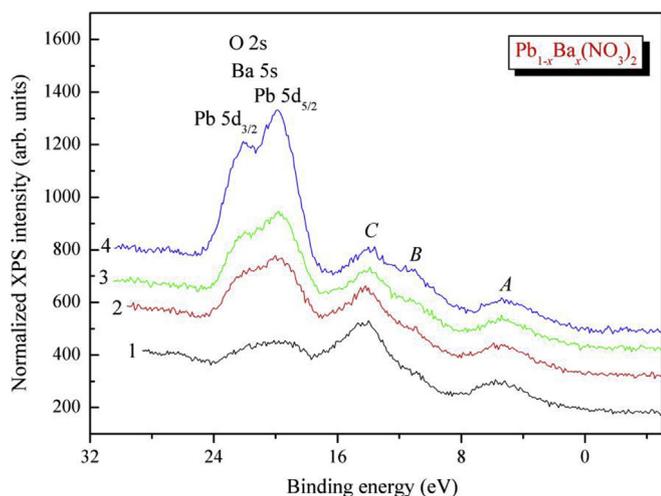
Fig. 5. XPS VB spectra (including some upper core levels) of $Pb_{1-x}Ba_x(NO_3)_2$ crystals: (1) $Pb_{0.19}Ba_{0.81}(NO_3)_2$, (2) $Pb_{0.42}Ba_{0.58}(NO_3)_2$, (3) $Pb_{0.68}Ba_{0.32}(NO_3)_2$ and (4) $Pb_{0.75}Ba_{0.25}(NO_3)_2$.

compounds [1,36], one could expect that in the $Pb_{1-x}Ba_x(NO_3)_2$ solid solutions the main input in the VB region should come from contributions of O 2p states. The energy distributions of the latter states can be evidenced from measurements of the X-ray emission O Kα band [37]. Results of the studies of this band of the $Pb_{1-x}Ba_x(NO_3)_2$ crystals are presented in Fig. 6. It is apparent that the O Kα bands in all $Pb_{1-x}Ba_x(NO_3)_2$ solid solutions under study are similar to each other: in addition to the main maximum 'a' positioned at about 523.5 eV, they reveal also a broad feature 'b' on its low-energy slope. We do not observe any significant changes in the energy positions of the maximum 'a' and the center of gravity of the band of the $Pb_{1-x}Ba_x(NO_3)_2$ crystals when altering the composition from $Pb_{0.19}Ba_{0.81}(NO_3)_2$ to $Pb_{0.75}Ba_{0.25}(NO_3)_2$ through the intermediate contents.

It is well known that the XPS and X-ray emission spectroscopy (XES) are very powerful techniques because their combination gives a possibility to probe experimentally peculiarities of the energy distribution of the valence electronic states and the occupation of the valence band in solids by electronic states of different symmetries originated from constituting atoms [12,37]. Therefore, in the present work we have made comparison of the XPS VB spectra and the X-ray emission O Kα bands on a common energy scale. For such a comparison, binding energy values of the O 1s core-level spectra (Table 3) of the $Pb_{1-x}Ba_x(NO_3)_2$ crystals have been taken into account as it is suggested to do in such a case [12,37]. Results of such a comparison of the XPS and XES data in the crystals under consideration are presented in Fig. 7. It is evident that the maximum 'a' of the X-ray emission O Kα bands of the $Pb_{1-x}Ba_x(NO_3)_2$ crystals is positioned at the top of the XPS VB spectra. Furthermore, the broad fine-structure peculiarity 'b' of the bands superimposes the lower portion of the sub-band A and upper portion of the sub-band B of the XPS

VB spectra. These data indicate that O 2p states contribute mainly at the top of the VB of the $Pb_{1-x}Ba_x(NO_3)_2$ crystals with also their substantial input in the upper and central portions of the band. The similar situation was detected previously in the case of the related compound, $K_2Ba(NO_3)_4$ [1]. Certainly, other valence electronic states of the constituting atoms (e.g., N p, Ba s,p, and Pb s,p states) should also give some contributions in the VB region of the $Pb_{1-x}Ba_x(NO_3)_2$ crystals. Such peculiarities can be clarified in future by using band-structure calculations of these crystals.

4. Conclusions

A series of solid solutions with a gradual increase in the volume and unit cell parameters from $Pb(NO_3)_2$ to $Ba(NO_3)_2$ is formed by the interaction of simple lead and barium nitrates. Earlier studies of $Pb_{0.67}Ba_{0.33}(NO_3)_2$ and $Pb_{0.33}Ba_{0.67}(NO_3)_2$ compounds found in the $Pb_{1-x}Ba_x(NO_3)_2$ system by McMurdie et al. [4] indicated that they belong to cubic noncentrosymmetric structure ($P2_13$), however Shtukenberg et al. [5] described a solid solution of $Pb_{1-x}Ba_x(NO_3)_2$ composition within

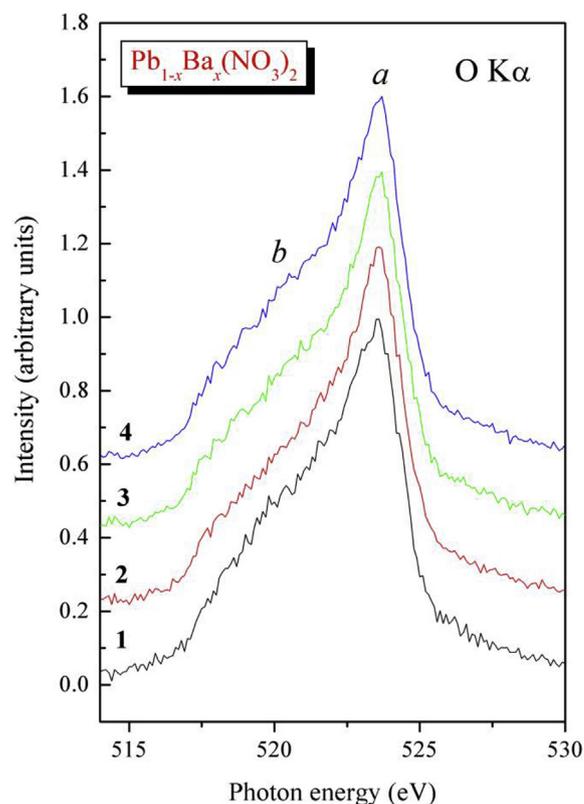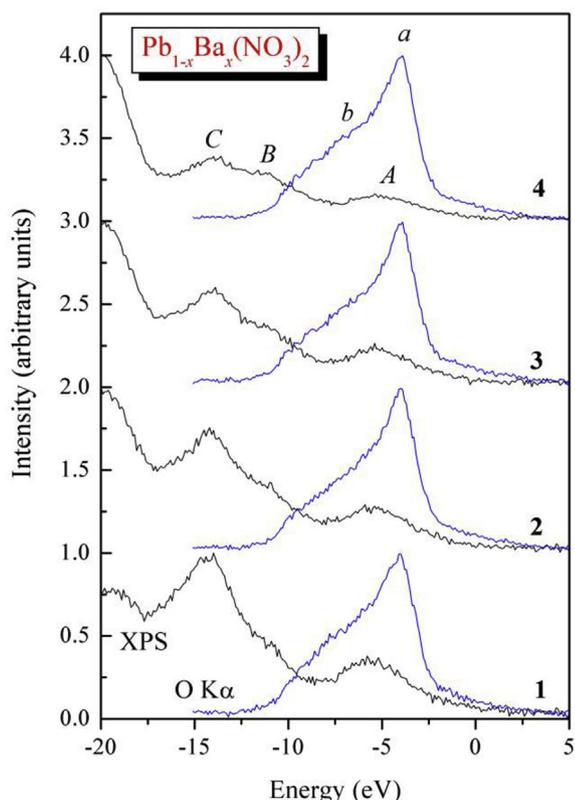**Fig. 6.** X-ray emission O Kα bands of $Pb_{1-x}Ba_x(NO_3)_2$ crystals: (1) $Pb_{0.19}Ba_{0.81}(NO_3)_2$, (2) $Pb_{0.42}Ba_{0.58}(NO_3)_2$, (3) $Pb_{0.68}Ba_{0.32}(NO_3)_2$ and (4) $Pb_{0.75}Ba_{0.25}(NO_3)_2$.

Table 3

Binding energies (in eV) of the core electrons of atoms constituting the $Pb_{1-x}Ba_x(NO_3)_2$ solid solutions (Note: precision of the measurements is ± 0.1 eV).

Core level	$Pb(NO_3)_2$	$Pb_{0.75}Ba_{0.25}$-$(NO_3)_2$	$Pb_{0.68}Ba_{0.32}$-$(NO_3)_2$	$Pb_{0.42}Ba_{0.58}$-$(NO_3)_2$	$Pb_{0.19}Ba_{0.81}$-$(NO_3)_2$	$Ba(NO_3)_2$
Pb $5d_{5/2}$	–	19.9	19.8	19.8	–	–
Pb $5d_{3/2}$	–	22.0	22.0	–	–	–
Ba $4d_{5/2}$	–	89.7	89.7	89.7	89.8	–
Ba $4d_{3/2}$	–	91.9	91.9	91.8	91.9	–
Pb $4f_{7/2}$	139.5	138.8	138.8	138.7	138.7	–
Pb $4f_{5/2}$	–	143.7	143.7	143.6	143.6	–
N 1s	407.4	406.9	406.9	406.9	407.0	407.1
O 1s	532.8	532.6	532.5	532.5	532.6	532.7
Ba $3d_{5/2}$	–	780.1	780.0	780.1	780.1	780.1-
Ba $3d_{3/2}$	–	795.5	795.4	795.4	795.5	–
Reference	[27]	This work	This work	This work	This work	[26]

Fig. 7. Comparison of the X-ray emission O Kα bands and the XPS VB spectra of $Pb_{1-x}Ba_x(NO_3)_2$ crystals on a general energy scale: (1) $Pb_{0.19}Ba_{0.81}(NO_3)_2$, (2) $Pb_{0.42}Ba_{0.58}(NO_3)_2$, (3) $Pb_{0.68}Ba_{0.32}(NO_3)_2$ and (4) $Pb_{0.75}Ba_{0.25}(NO_3)_2$.

trigonal centrosymmetric structure (R-3). The present refinement of the $Pb_{1-x}Ba_x(NO_3)_2$ solid solution indicates that the crystal structure of all obtained $Pb_{1-x}Ba_x(NO_3)_2$ crystals belong to a cubic space group *Pa*-3, with the parameter *a* ranging from 7.956(3) to 8.096(6) Å, while *V* ranging from 503.615(3) to 530.68(1) Å^3. In this series, all structures are built on the basis of barium nitrate structure and have the same construction, where lead cation occupies barium positions. The lattice is characterized by the same cation coordination number (12) and the only equilateral NO_3 triangle. In this case, the change in bond lengths is irregular in the series going from $Pb(NO_3)_2$ to $Ba(NO_3)_2$. It should be indicated the Pb^{2+} ion has a lone pair of electrons that are likely to be stereochemically active in these solid solutions. This may lead to a significant amount of local disorder which explains the spread in the lattice parameters of the $Pb_{1-x}Ba_x(NO_3)_2$ crystals under consideration.

The grown $Pb_{1-x}Ba_x(NO_3)_2$ crystals have been characterized in the present work by using XPS and XES techniques. The XPS data indicate that all features are well ascribed to the core-levels and Auger lines of the chemical elements constituting the $Pb_{1-x}Ba_x(NO_3)_2$ crystals. We do not observe any visible changes in magnitudes of the SO splitting of XPS core-level Ba 3d(4d) and Pb 4d(4f) spectra when changing the composition of the $Pb_{1-x}Ba_x(NO_3)_2$ crystals from $Pb_{0.19}Ba_{0.81}(NO_3)_2$ to $Pb_{0.75}Ba_{0.25}(NO_3)_2$ through the intermediate contents. The present XPS data allow for statement that the substitution of lead for barium does not lead to changes in the charge states of the atoms constituting the $Pb_{1-x}Ba_x(NO_3)_2$ crystals. The binding energy values of the XPS N 1s core-level spectra being in the range of $(406.9–407.0)\pm0.1$ eV are found to be significantly higher as compared with those of nitrides based on transition metals as well as inorganic nitrogen-containing compounds, while the binding energy magnitudes of the O 1s spectra in the $Pb_{1-x}Ba_x(NO_3)_2$ solid solutions $((532.5–532.6)\pm0.1$ eV) are also much bigger as compared with those of the O 1s electrons in transition metal oxides as well as in BaO and PbO_2. Comparison of the XPS VB spectra and the X-ray

emission O Kα bands on a common energy scale indicates that O 2p states contribute mainly at the top of the valence band of the $Pb_{1-x}Ba_x(NO_3)_2$ crystals with also their substantial input in the upper and central portions of the band.

References

[1] L.I. Isaenko, K.E. Korzhneva, S.V. Goryainov, A.A. Goloshumova, L.A. Sheludyakova, V.L. Bekenev, O.Y. Khyzhun, Structural, optical and electronic properties of $K_2Ba(NO_3)_4$ crystal, Physica B 531 (2018) 149–158.

[2] Guohong Zou, Chensheng Lin, Hyung Gu Kim, Hongil Jo, Ok Kang Min, $Rb_2Na(NO_3)_3$: a congruently melting UV-NLO crystal with a very strong second harmonic generation response, Crystals 6 (2016) 42.

[3] B.D. Stepin, Z.A. Starikova, A.N. Knyazeva, G.A. Lovetskaya, V.K. Trunov, Solid solutions KNO_3-$RbNO_3$-H_2O and $CsNO_3$-$RbNO_3$-H_2O, J. Inorg. Chem. 23 (1978) 126–128.

[4] H.F. McMurdie, M.C. Morris, et al., Standard X-Ray Diffraction Powder Pattern: Monograph, Institute for Materials Research, National Bureau of Standards, Washington, 1975, p. 96.

[5] A.G. Shtukenberg, H. Euler, A. Kiefel, D.Y. Popov, Symmetry reduction and cation ordering in solid solutions of strontium–lead and barium–lead nitrates, Z. Kristallogr. 221 (10) (2006) 681–688.

[6] Bruker AXS TOPAS V4, General Profile and Structure Analysis Software for Powder Diffraction Data, User's Manual, Bruker AXS), Karlsruhe, Germany, 2008.

[7] V.E. Henrich, P.A. Cox, The Surface Science of Metal Oxides, Cambridge University Press, Cambridge, 1994.

[8] M.Y. Rudysh, M.G. Brik, O.Y. Khyzhun, A.O. Fedorchuk, I.V. Kityk, P.A. Shchepanskyi, V.Y. Stadnyk, G. Lakshminarayana, R.S. Brezvin, Z. Bak, M. Piasecki, Ionicity and birefringence of α-LiNH$_4$SO$_4$ crystals: ab initio DFT study, X-ray spectroscopy measurements, RSC Adv. 7 (2016) 6889–6901.

[9] M.Y. Rudysh, M.G. Brik, V.Y. Stadnyk, R.S. Brezvin, P.A. Shchepanskyi, A. Fedorchuk, O.Y. Khyzhun, I.V. Kityk, M. Piasecki, Ab initio calculations of the electronic structure and specific optical features of β-LiNH$_4$SO$_4$ single crystals, Physica B 528 (2018) 37–46.

[10] V.V. Atuchin, V.L. Bekenev, O.D. Chimitova, M.S. Molokeev, B.G. Bazarov, J.G. Bazarova, O.Y. Khyzhun, C.S. Lim, Synthesis and electronic properties of β-RbNd(MoO$_4$)$_2$, Asian J. Chem. 26 (2014) 1284–1286.

[11] S.F. Solodovnikov, V.V. Atuchin, Z.A. Solodovnikova, O.Y. Khyzhun, M.I. Danylenko, D.P. Pishchur, P.E. Plyusnin, A.M. Pugachev, T.A. Gavrilova, A.P. Yelisseyev, A.H. Reshak, Z.A. Alahmed, N.F. Habubi, Synthesis, structural, thermal, and electronic properties of palmierite-related double molybdate α-Cs$_2$Pb(MoO$_4$)$_2$, Inorg. Chem. 56 (2017) 3276–3286.

[12] A. Meisel, G. Leonhardt, R. Szargan, X-Ray Spectra and Chemical Binding, Springer-Verlag, Berlin/Heidelberg, 1989.

[13] H. Nowotny, G. Heger, Structure refinement of strontium nitrate, Sr(NO$_3$)$_2$, and barium nitrate, Ba(NO$_3$)$_2$, Acta Crystallogr. Sect. C Cryst. Struct. Commun. 39 (1983) 952–956.

[14] Paul B. Moore, Pradip K. Sen Gupta, Elmer O. Schlemper, Solid solution in plumbous potassium oxysilicate affected by interaction of a lone pair with bond pairs, Nature 318 (1985) 548–550.

[15] Paul Brian Moore, Pradip K. Sen Gupta, Jinchuan Shen, Elmer O. Schlemper, The kentrolite-melanotekite series, 4Pb2(Mn,Fe)23++O2[Si2O7]: chemical crystallographic relations, lone-pair splitting, and cation relation to 8URe2, Am. Mineral. 76 (1991) 1389–1399.

[16] Pradip K. Paul Brian Moore, Sen Gupta, Yvon Le Page, Magnetoplumbite, Pb2+ Fe3 +12O19: refinement and long-pair splitting, Am. Mineral. 74 (1989) 1186–1194.

[17] G.R. Bulka, N.M. Nizamutdinov, N.M. Nazarova, Dissymmetrization of crystals: theory and experiment, Phys. Chem. Menerals 6 (1980) 283–293.

[18] L.I. Tsinober, M.I. Samoylovich, Distribution of structural defects and anomalous optical symmetry in quartz crystals, in: B.K. Vainshtein, A.A. Chernov (Eds.), Problems of Modern Crystallography, Nauka, Moscow, 1975, pp. 207–218.

[19] P. Gopalan, M. Peterson, G. Crundwell, B. Kahr, Reevaluating structures for mixed crystals of simple isomorphous salts: sodium chlorate bromate (NaCl$_x$Br$_{1-x}$O$_3$), J. Am. Chem. Soc. 115 (1993) 3366–3367.

[20] G. Crundwell, P. Goplan, A. Bakulin, M.L. Peterson, B. Kahr, Effect of habit modification on optical and X-ray structures of sodium halite mixed crystals: the etiology of anomalous double refraction, Acta Crystallogr. B 53 (1997) 189–202.

[21] A.G. Shtukenberg, I.V. Rozhdestvenskaya, D.Y. Popov, Y.O. Punin, Kinetic ordering of atoms in sodium chlorate-bromate solid solutions, J. Solid State Chem. 177 (2004) 4732–4742.

[22] A.G. Shtukenberg, Y.O. Punin, E. Haegele, H. Klapper, On the origin of inhomogeneity of anomalous birefringence in mixed crystals: an example of alums, Phys. Chem. Miner. 28 (2001) 665–674.

[23] M. Akizuki, M.C. Hampar, J. Zussman, An explanation of anomalous optical properties of topaz, Mineral. Mag. 43 (1979) 237–241.

[24] A.G. Shtukenberg, D.Y. Popov, Y.O. Punin, Growth ordering and anomalous birefringence in ugrandite garnets, Mineral. Mag. 69 (2005) 537–550.

[25] A.G. Shtukenberg, Metastability of atomic ordering in lead-strontium nitrate solid solutions, J. Solid State Chem. 178 (2005) 2608–2612.

[26] R.P. Vasquez, X-ray photoelectron spectroscopy study of Sr and Ba compounds, J. Electron. Spectrosc. Relat. Phenom. 56 (1991) 217–240.

[27] J.A. Taylor, G.M. Lancaster, J.W. Rabalais, Chemical reactions of N_2^+ ion beams with group IV elements and their oxides, J. Electron. Spectrosc. Relat. Phenom. 13 (1978) 435–444.

[28] C.D. Wagner, W.M. Riggs, L.E. Davis, J.F. Moulder, G.E. Muilenberg (Eds.), Handbook of X-Ray Photoelectron Spectroscopy, Perkin-Elmer Corp., Phys. Elect. Div., Minnesota, 1979.

[29] D. Briggs, P.M. Seach (Eds.), Practical Surface Analysis (2nd Ed.): Vol. 1: Auger and X-Ray Photoelectron Spectroscopy, John Willey & Sons Ltd., Chichester, 1990.

[30] V.I. Nefedov, X-Ray Electron Spectroscopy of Chemical Compounds, Khimiya, Moscow, 1984.

[31] D.N. Hendrickson, J.M. Hollander, W.L. Jolly, Nitrogen 1s electron binding energies. Correlations with molecular orbital calculated nitrogen charges, Inorg. Chem. 8 (1969) 2642–2647.

[32] B. Folkesson, ESCA studies on the charge distribution in some dinitrogen complexes of rhenium, iridium, ruthenium, and osmium, Acta Chem. Scand. 27 (1969) 287–302.

[33] O.Y. Khyzhun, T. Strunskus, Y.M. Solonin, XES, XPS and NEXAFS studies of the electronic structure of cubic $MoO_{1.9}$ and $H_{1.63}MoO_3$ thick films, J. Alloy. Comp. 366 (2004) 54–60.

[34] S. Hüfner, Photoelectron Spectroscopy: Principles and Applications, third ed., Springer-Verlag, Berlin/Heidelberg, 2003.

[35] O.Y. Khyzhun, V.L. Bekenev, N.M. Denysyuk, L.I. Isaenko, A.P. Yelisseyev, A.A. Goloshumova, A.Y. Tarasova, Specific peculiarities of the electronic structure of $SrPb_3Br_8$ as evidenced from first-principles DFT band-structure calculations, J. Electron. Mater. 48 (2019) 3059–3068.

[36] O. Karslıoğlu, L. Trotochaud, I. Zegkinoglou, H. Bluhm, X-ray spectroscopic characterization of BaO, Ba(OH)$_2$, BaCO$_3$, and Ba(NO$_3$)$_2$, J. Electron. Spectrosc. Relat. Phenom. 225 (2018) 55–61.

[37] S. Rajagopal, D. Nataraj, O.Y. Khyzhun, Y. Djaoued, J. Robichaud, K. Senthil, D. Mangalaraj, Systematic synthesis and analysis of change in morphology, electronic structure and photoluminescence properties of pyrazine intercalated MoO_3 hybrid nanostructures, CrystEngComm 13 (2011) 2358–2368.